Nanotechnology Perceptions
ISSN 1660-6795
www.nano-ntp.com

Myriophyllum Sibiricum Plant-Based Zinc Oxide Nanoparticles for Photocatalytic Reduction of Hexavalent Chromium

Opeyemi A. Oyewo[1], Seshibe S. Makgato[1], Damian C. Onwudiwe[2,3]

[1]Department of Chemical Engineering, College of Science, Engineering and Technology, University of South Africa (UNISA), c/o Christian de wet & Pioneer Avenue, Florida Campus 1710, Johannesburg, South Africa
[2]Materials Science Innovation and Modelling (MaSIM) Research Focus Area, Faculty of Natural and Agricultural Sciences, North-West University, Mafikeng Campus, Private Bag X2046, Mmabatho, 2735, South Africa
[3]Department of Chemistry, School of Physical and Chemical Sciences, Faculty of Natural and Agricultural Sciences, North-West University, Mafikeng Campus, Private Bag X2046, Mmabatho, 2735, South Africa
Email: Atiba.opeyemi@gmail.com

The synthesis of Myriophyllum sibiricum plant-based Zinc oxide nanoparticles was investigated via the co-precipitation method, and they were found to be effective for reducing Cr(VI) ions in aqueous solution. The formation of ZnO nanoparticles was confirmed by various techniques including X-ray diffraction, scanning electron microscopy, transmission electron microscopy, and UV-visible absorption spectroscopy. The results showed that 25 and 30 mL of the plant extract (ZnO-25 and ZnO-30) produced hexagonal phase and highly crystalline ZnO nanoparticles with spherical morphology and an average particle size of 17.92 and 21.14 nm, respectively. The ZnONPs were used in the photo-enhanced reduction of hexavalent Cr ions, and the effects of solution pH, starting metal concentrations, and photocatalyst dosage were studied to determine the maximum performance of biogenic. ZnO-30 also demonstrated better free radical scavenging activity than ZnO-25. Using 2 g/L of ZnO nanoparticles resulted in a maximum Cr(VI) reduction of 90.2%. The results showed a clear relationship between metal ion reduction and catalyst dosage, with 2 g of ZnO nanoparticles. This demonstrates that biogenic synthesized ZnO nanoparticles are a promising photocatalyst capable of converting Cr(VI) into less hazardous Cr(III). These results, in accord with recent research indicating green approaches, are more

effective in developing metal oxide nanoparticles and demonstrating higher photocatalytic activity.

Keywords: Biogenic, chromium(VI);,Free radicals, Myriophyllum sibiricum, ZnO nanoparticles.

1. Introduction

Zinc oxide nanoparticles are the most frequent nanoparticles among metal oxides [1, 2], and they are distinguished by their broad band gap n-type semiconductor characteristics. It is non-toxic, highly durable, and has improved thermal and chemical stability[2]. Furthermore, ZnONPs are cost-effective, naturally abundant, possess a single oxidation state, and are highly biocompatible[3]. These properties make them an excellent choice for different industrial applications. The widespread usage of nanoparticles in modern medicine has been linked to their unique interaction with biological cells, specifically their penetration of cell walls and disruption of biochemical pathways[4]. Also, the broadband gap energy associated with ZnONPs rendered it an excellent and highly efficient catalyst in water treatment applications via photocatalysis technique[5].

The traditional synthesis of ZnO NPs frequently uses energy-intensive procedures with dangerous substances, which thus causes harm to the environment. To alleviate this issue, plant-based synthesis of ZnO NPs has become a viable and environmentally friendly solution[4, 6]. This is because utilizing plant extracts as stabilizing and reducing agents guarantees a biocompatible and environmentally benign procedure which is the purpose of this work. However, a thorough feasibility study is required to determine the appropriate plant with the needed properties.

In this context, Myriophyllum sibiricum, a submerged aquatic plant with a rich phytochemical profile, provides a novel platform for the environmentally friendly synthesis of ZnO NPs in this regard[7]. The bioactive substances found in the plant, such as tannins, phenolics, and flavonoids, are essential for stabilizing the nanoparticles and lowering zinc ions. These biosynthesized ZnO NPs exhibit remarkable photocatalytic properties, making them an effective agent for the removal of water pollutants. They are capable of utilizing light energy to drive redox reactions, making them suitable for the reduction of Cr(VI) to its less toxic trivalent form (Cr(III)[8].

Cr(VI) is one of the five heavy metals flagged by WHO due to its severe health and environmental effects[9]. Hexavalent chromium is a known carcinogen and mutagen, it is extensively used in industries like leather tanning, electroplating, and pigment production, resulting in its persistent contamination in the environment[10]. Developing effective and sustainable strategies for its removal has thus become a critical challenge. In our previous study[11], a similar plant (Myriophyllum spicatum) was utilized for the synthesis of an efficient CuO for the reduction of Cr(VI) to Cr(III), the outcome of this research suggested the robustness of this plant and its species. It is hereby speculated that the biogenic ZnONPs can efficiently reduce Cr(IV) to less harmful Cr(III) for further industrial reuse.

Consequently, this study explores the biogenic synthesis, characterization, and photocatalytic efficiency of Myriophyllum sibiricum-derived ZnO nanoparticles in reducing Cr(VI) under

light irradiation. The work provides a sustainable way to manage environmental pollution while developing green nanotechnology practices by fusing the sophisticated capabilities of green nanotechnology with the natural phytochemistry of the plant.Materials and methods

2. Materials and Methods

2.1 Materials

Fresh leaves of Myriophyllum spicatum were gathered from the Vaal River in South Africa and identified correctly. The initial pH was changed using 0.1 M HCl and NaOH. We bought lead nitrate salts, potassium dichromate, and copper acetate from Sigma-Aldrich in South Africa. The Model Select Analyst HP40, a piece of equipment made in the United Kingdom, processed the deionized water used to prepare the solution. Every chemical that was used was analytical grade.

2.2 Methods

2.2.1 Preparation of Myriophyllum spicatum leaf extract

Myriophyllum spicatum leaves were double-washed with purified water to remove the adhering dirt and then shade-dried for 7 days [12, 13]. About 8 g of blended leaves were added to 80 mL of deionized water and was then heated at 70 ℃ for 5 h. The mixture was then filtered and cooled to 25 ℃ before storing in a refrigerator.

2.2.2 Synthesis of ZnO nanoparticles

The techniques outlined by Ghorbani, Mehr [14] were used to synthesize the biogenic ZnO nanoparticles. However, 15, 20, 25 and 30 mL of the extract were utilized to synthesize Myriophyllum spicatum-based ZnONPs, the optimum volumes of 25 and 30 mL extract designated as ZnO-25 and ZnO-30 nanoparticles. Essentially, each of 25 and 30 mL of plant extracts were combined with 20.05 mL of zinc acetate solution. To bring the pH down to 7, a NaOH solution was utilized. These mixtures were then agitated with a magnetic stirrer in a beaker at 85°C for two hours. The solutions were centrifuged for 15 minutes at 5000 rpm, and the supernatant was disposed of. After being cleaned using a 1:1 ethanol and distilled water mixture, the leftover product was centrifuged three times to get rid of any contaminants. Afterwards, the product was dried overnight in a fume hood and then calcined at 400 ℃ for 2 h to afford a white product which was later characterized to confirm the successful synthesis of biogenic ZnO nanoparticles.

2.2.3 Characterization of nanoparticles

A Bruker D8 Advanced X-ray diffractometer (Karlsruhe, Germany) with a proportional counter that uses Cu Kα radiation (k = 1.5405 Å; nickel filter), was used to identify the phase and crystalline nature of the biogenic ZnO nanoparticles. A Quanta FEG 250 scanning electron microscope (SEM) with a 30 kV acceleration voltage was used for the analysis of the external morphology. A TECNAI G2 (ACI) transmission electron microscope (TEM) with a 200 kV accelerating voltage was used to examine the internal morphology of the ZnO nanoparticles. The absorption property of the synthesized ZnO nanoparticles was measured using a Cary 30 UV-vis spectrophotometer (Agilent Technologies from 200 to 800 nm).

2.2.4. Photocatalytic reduction of Cr(VI) in water

The reduction of the Cr(VI) ions in simulated water was investigated using plant-based ZnO nanoparticles under visible light irradiation. For this investigation, a 250–W Xe discharge lamp was used with a flowing water source inside the reactor vessel. In this investigation, 0.5 to 2 g of ZnO nanoparticles and a concentration of roughly 50 mg/L of metal ions were utilized. After adding the nanoparticles to the aqueous pollutant solution, it was magnetically agitated for an hour in the dark until the adsorption equilibrium was achieved. After that, the mixture was continuously stirred for 120 minutes while exposed to a visible lamp. The aliquots were taken from the solution at 15-minute intervals over a 120-minute time. The degradation efficiency of the chromium ions was studied using UV–visible spectrophotometer

The percentage photocatalytic reduction of Cr(VI) ions was calculated using the following equation:

$$\text{Reduction yield \%} = \frac{C_o - C_e}{C_o} \times 100 \quad (1)$$

Where, C_0 is the initial concentration C_e is the concentration of metals after a specific time.

3. Results and discussions

3.1 Characterization results

3.1.1 X-ray diffraction studies of biogenic ZnO nanoparticles

Figures 1a-d depict the diffraction patterns of ZnO-15, ZnO-20, ZnO-25, and ZnO-30 nanoparticles, based on the volume of extract utilized in the synthesis. The diffraction patterns of ZnO-25 and ZnO-30 nanoparticles showed a high degree of crystallinity, comparable to recent findings in the literature [5]. The diffraction peaks for ZnO-25 and ZnO-30 appeared at 2θ values of 32.01°, 34.67°, 36.46°, 47.75°, 56.79°, 63.04°, 67.52°, 68.14°, 69.25º, 72.73º, 77.14º, 81.57°, and 31.93°, 34.57°, 36.38°, 47.63°, 56.67°, 62.89°, 67.51°, 68.0°, 69.12º, 72.56º. 76.98º, 82.12° are in good agreement with a hexagonal wurtzite structure (JCP2 card no. 36-1451) with a lattice constant of a = b = 3.242 Å and c = 5.205 Å [15]. Debye-Scherer equation (Equation 2) was used to estimate the average crystallite size of both ZnO-25 and ZnO-30 nanoparticles [16] and the size of the nanoparticles was found to be about 19.45 and 24.60 nm, respectively.

$$D = \frac{K\lambda}{\beta \cos\theta} \quad (2)$$

Where, D = crystallite size (nm), K = 0.9 (Scherrer constant), λ = 0,15406 Å, β = Full width at half maximum (FWHM), and θ = Bragg's angle of reflection.

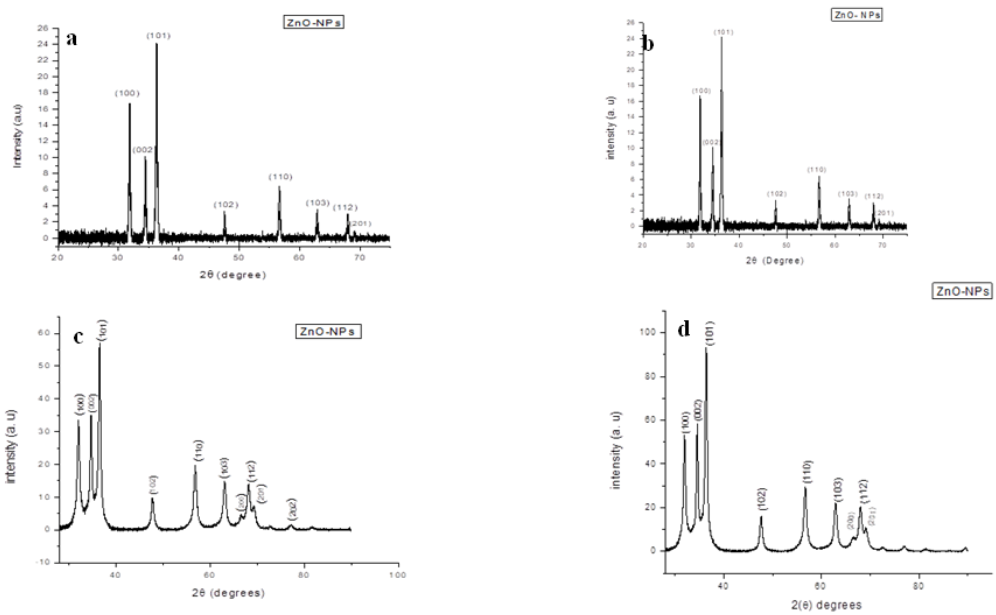

Figure 1: X-ray diffraction studies of Myriophyllum spicatum plant extract ZnONPs (a)15 mL (b) 20 mL (c) 25 mL (d) 30 mL

3.1.2 SEM, TEM, and particle size distribution of biogenic ZnO nanoparticles

Figure 2a–f shows the morphological properties of ZnO-25 and ZnO-30 nanoparticles. SEM micrographs of ZnO-25 and ZnO-30 revealed a spherical form with a high degree of agglomeration (Fig. 2a and b). This mass gathering of nanoparticles could be attributed to particle contact caused by substantial kinetic energy from high-temperature calcination [8]. Furthermore, the large agglomerations may be owing to the creation of metallic connections that are difficult to rupture, therefore, increasing the surface reactivity [17]. The interior morphology of these samples is shown in Figures 2c and 2d which also confirm that ZnO-25 and ZnO-30 nanoparticles have a spherical form with some aggregation on their surfaces. The particle sizes of ZnO-25 and ZnO-30 (Fig. 3a and f) were determined to be 18.02 and 21.11 nm.

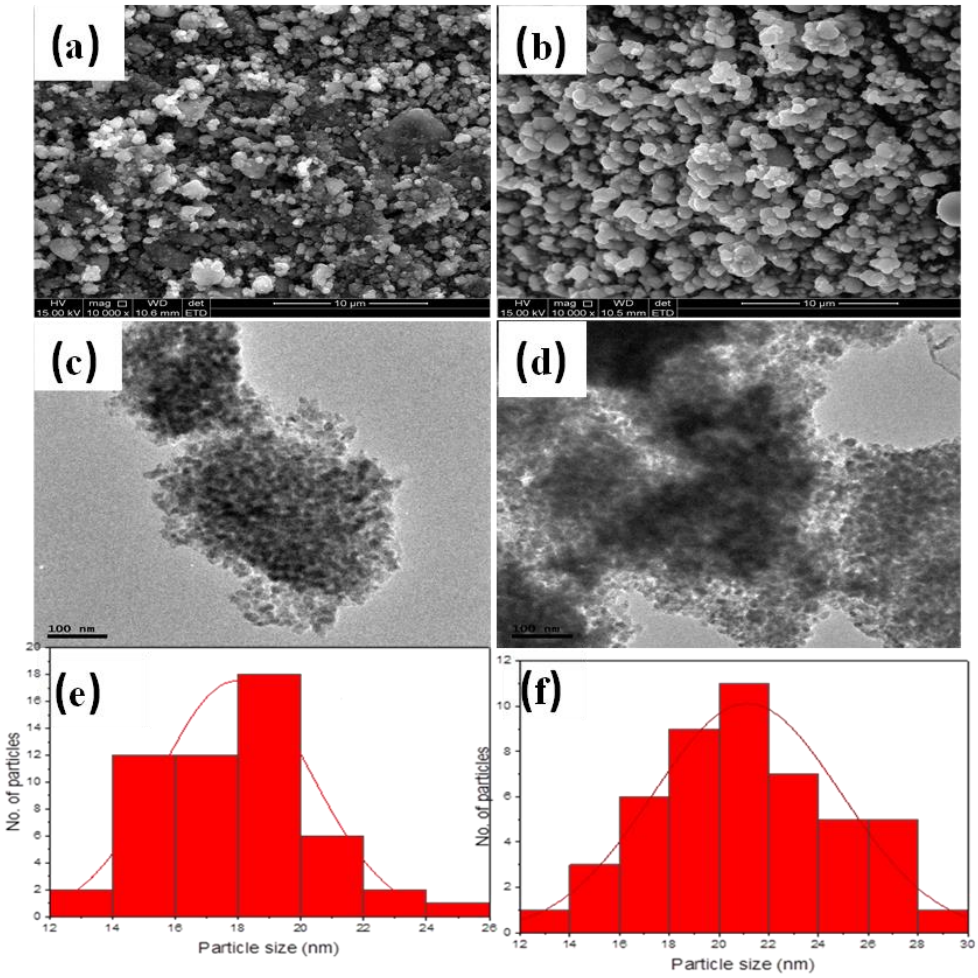

Figure 2: (a, b) SEM of ZnO-25 and ZnO-30 mL, (c, d) TEM of ZnO-25 and ZnO-30mL (e, f) particle size distribution histogram of ZnO-25 and ZnO-30 mL of the extract of Myriophyllum spicatum plant -ZnONPs

3.1.3 UV-visible studies of ZnO nanoparticles synthesized using Myriophyllum spicatum extract

The UV-visible absorption spectra of ZnO-25 and ZnO-30 show a strong absorption peak at 375 and 378 nm, consistent with ZnO. These peaks confirm the successful production of biogenic ZnO nanoparticles and could be attributed to inherent electron transmissions from ZnO's valence band to the conduction band [10]. Similar results were reported for ZnO nanoparticles produced from Caesalpinia crista [18] and Artocarpus hirsutus [19]. The band-gap energies of both ZnO nanoparticles were determined using Tauc's plot equation (equation 3).

$$\alpha h\nu = [A(h\nu - Eg)]^n \quad (3)$$

where α is the absorption coefficient, A is the constant, h is the plank's constant, ν is the photon frequency, Eg is the optical band gap energy, and n is 1/2 for direct band gap semiconductor.

The computed band gap energies for ZnO-25 and ZnO-30 nanoparticles were 3.25 (Fig. 3b) and 3.31 eV (Fig. 3d). These results are slightly lower than bulk ZnO's band gap of 3.4 eV.

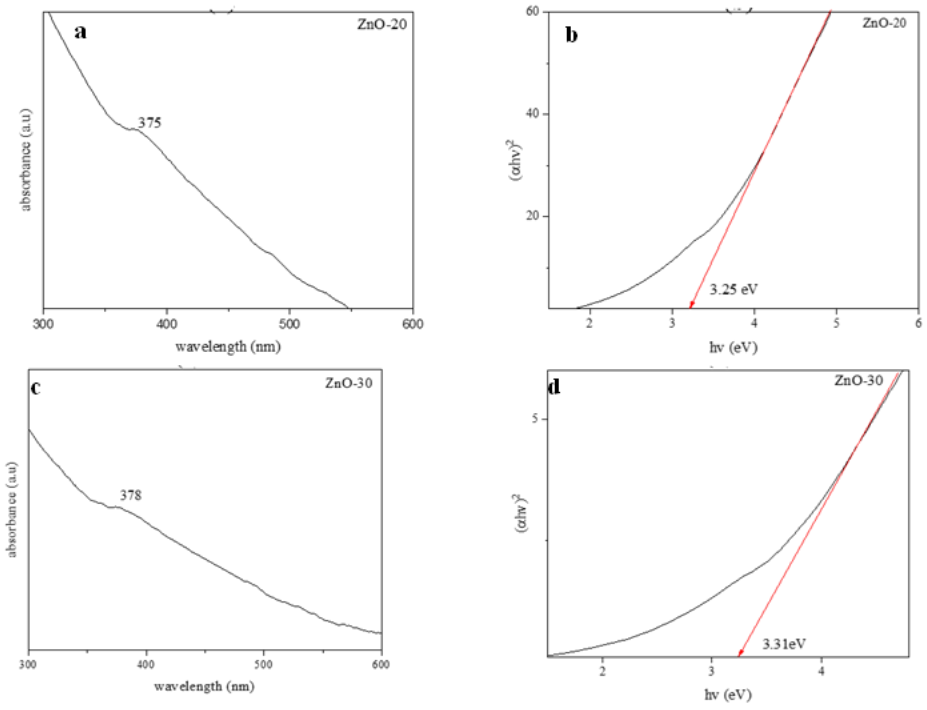

Figure 3: UV-vis: (a) Absorption spectrum, and (b) Tauc plot of ZnO-25 mL (c) Absorption spectrum, and (b) Tauc plot of ZnO-30.

3.2 . Photocatalyst reduction of Cr(VI) to Cr(III)

Hexavalent chromium exists in three ionic forms: HCrO4−, CrO4, and Cr2O72− [20]. These species are predominated in different solution pH, chromium ions exist in both neutral and basic media, while the hydro chromium can be found in lower pHs. The amount of Cr(VI) remaining at any given time was calculated using the relationship:

$$[\mathrm{Cr}_{(\mathrm{Tot})}] - [\mathrm{Cr(VI)}] = [\mathrm{Cr(III)}], \quad (4)$$

$$\frac{[\mathrm{Cr}_{(\mathrm{Tot})}] - [\mathrm{Cr(VI)}]}{[\mathrm{Cr}_{(\mathrm{Tot})}]} \quad (5)$$

The reduction of Cr(VI) to Cr(V), by reducing the molecular oxygen to hydrogen peroxide is the first stage in the reduction procedure of Cr(VI) to Cr(III). After that, Cr(V) generates hydroxyl radicals, followed by intermediates like Cr(IV), free radicals, and finally Cr(III) [21, 22].

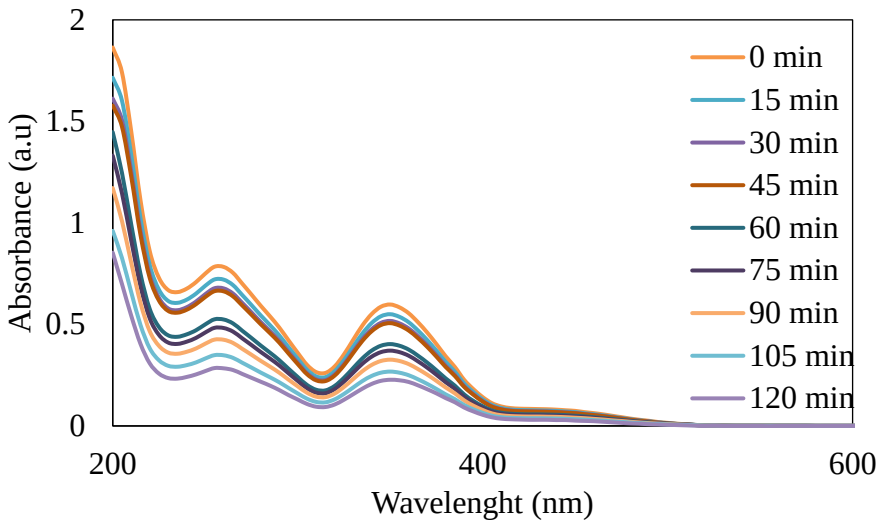

Figure 4: UV-vis absorption spectra of photocatalytic reduction of Cr(VI) ions using biogenic ZnONPs

3.3 The effects of solution pH on the Cr(VI) and Pb(II) reduction

The pH of the solution determines the impact of surface charges, which are positive in acidic environments and negative in alkaline environments. Figure 5 depicts the effect of solution pH on the photocatalytic reduction of Cr(VI). As such, Cr(VI) solution pH between 3 and 9 was tested on biogenic ZnO nanoparticles. Acidic mediums reduce Cr(VI) to Cr(III) than alkaline mediums. As the pH increases, the reduction of Cr(VI) metal ions decreases, which might be attributed to a decrease in the number of H+ ions in the solution. The electrostatic interaction between positively charged metal ions and negatively charged nanoparticles is thought to be the primary mechanism controlling Cr ion reduction in water. As a result, the fate of Cr(VI) during photocatalytic reduction is determined by the surface charge at the semiconductor-electrolyte interface.

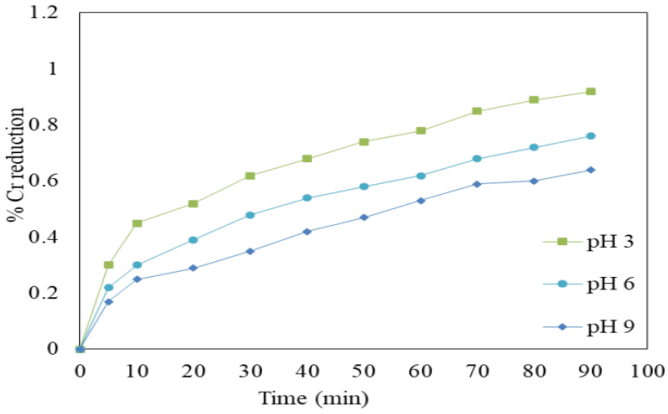

Figure 5: Effect of solution pH on the reduction of Cr(VI) using an extract of Myriophyllum

spicatum-based ZnONPs (conc of photocatalyst =2 g/L, Cr(VI)=50 mg/L).

3.4 Effect of the catalyst dosage and initial concentration of Cr(VI)

Metal ion concentrations ranged from 20 to 80 mg/L, and catalyst dosages of 0.5 to 2 g/L were studied. Figures 6a and 6b show how various process parameters affect the reduction of Cr(VI) to Cr(III). An indirect link between concentration rise and the rate of reduction of the metal ion was discovered. This could be because the large concentration of metal ions slowed the migration of both ions to the semiconductor surface. On the other hand, increasing the catalyst dosage resulted in a greater reduction of metal ions in the solution. This suggested an increase in the active site of the catalyst in the solution as the ZnO dosage increased, which improved the reduction process in water [23]

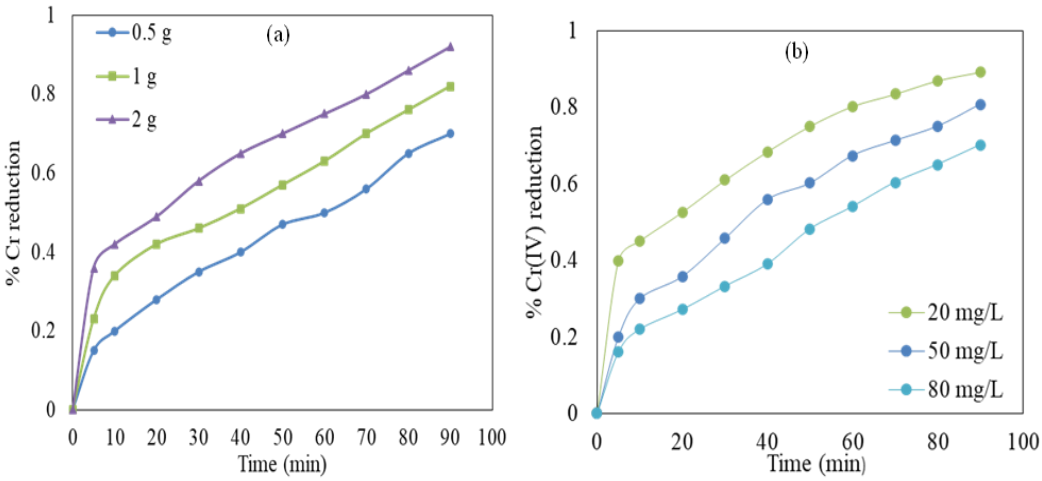

Figure 6: Effect (a) catalyst dose (b) Cr(VI) initial concentration using an extract of Myriophyllum spicatum-based ZnONPs (conc of photocatalyst =2 g/L, Cr(VI)=20 mg/L).

4. Conclusion

ZnO nanoparticles were successfully produced utilizing various amounts of Myriophyllum spicatum plant extract to reduce Cr(VI) to Cr(III). The physicochemical properties of biogenic ZnO nanoparticles were studied with XRD, SEM, TEM, and UV-visible absorption techniques. X-ray diffraction examination revealed that 25 and 30 mL ZnO nanoparticles based on Myriophyllum spicatum plant extract had a higher crystallinity and a hexagonal wurtzite structure. The internal and external morphology showed both nanoparticles to be spherical with average particle sizes of 18.02 and 21.11 nm for ZnO-25 and ZnO-30. The photocatalytic analysis revealed that plant-based ZnO nanoparticles reduced Cr(VI) with a better efficiency of 90.2%. As the pH rose from 3 to 9, the reduction efficiency dropped. An increase in the catalyst dosage was discovered to be directly proportional to the reduction to Cr(VI), but a rise in the concentration of Cr(VI) inhibited the removal process.

Acknowledgement

The author would like to acknowledge the Department of Chemical Engineering, College of Science, Engineering and Technology, University of South Africa, and National Research Foundation (Grant No: 151158), South Africa for financial support.

References

1. Ischenko, V., et al., Zinc oxide nanoparticles with defects. Advanced functional materials, 2005. 15(12): p. 1945-1954.
2. Sirelkhatim, A., et al., Review on zinc oxide nanoparticles: antibacterial activity and toxicity mechanism. Nano-micro letters, 2015. 7: p. 219-242.
3. Jiang, J., J. Pi, and J. Cai, The advancing of zinc oxide nanoparticles for biomedical applications. Bioinorganic chemistry and applications, 2018. 2018(1): p. 1062562.
4. Bhuyan, T., et al., Biosynthesis of zinc oxide nanoparticles from Azadirachta indica for antibacterial and photocatalytic applications. Materials Science in Semiconductor Processing, 2015. 32: p. 55-61.
5. Balcha, A., O.P. Yadav, and T. Dey, Photocatalytic degradation of methylene blue dye by zinc oxide nanoparticles obtained from precipitation and sol-gel methods. Environmental Science and Pollution Research, 2016. 23: p. 25485-25493.
6. Bhattacharjee, N., et al., A critical review on novel eco-friendly green approach to synthesize zinc oxide nanoparticles for photocatalytic degradation of water pollutants. International Journal of Environmental Analytical Chemistry, 2024. 104(3): p. 489-516.
7. Glisson, W.J. and D.J. Larkin, Hybrid watermilfoil (Myriophyllum spicatum × Myriophyllum sibiricum) exhibits traits associated with greater invasiveness than its introduced and native parental taxa. Biological Invasions, 2021. 23(8): p. 2417-2433.
8. Shnawa, B., et al., Scolicidal activity of biosynthesized zinc oxide nanoparticles by Mentha longifolia L. leaves against Echinococcus granulosus protoscolices. Emergent Materials, 2021. 5.
9. Vardhan, K.H., P.S. Kumar, and R.C. Panda, A review on heavy metal pollution, toxicity and remedial measures: Current trends and future perspectives. Journal of Molecular Liquids, 2019. 290: p. 111197.
10. Huang, Y., et al., Facile synthesis of sodium lignosulfonate/polyethyleneimine/sodium alginate beads with ultra-high adsorption capacity for Cr (VI) removal from water. Journal of Hazardous Materials, 2022. 436: p. 129270.
11. Oyewo, O.A. and S.S. Makgato, Photocatalytic Reduction of Cr (VI) and Pb (II) with Biogenically Synthesized Copper Oxide Nanoparticles Using an Extract of the Myriophyllum spicatum Plant. J, 2023. 6(4): p. 564-578.
12. Chauhan, M., et al., Green synthesis of CuO nanomaterials and their proficient use for organic waste removal and antimicrobial application. 2019. 168: p. 85-95.
13. Hassan, S.E.-D., et al., Endophytic actinomycetes Streptomyces spp mediated biosynthesis of copper oxide nanoparticles as a promising tool for biotechnological applications. 2019. 24: p. 377-393.
14. Ghorbani, H.R., et al., Synthesis of ZnO nanoparticles by precipitation method. Orient. J. Chem, 2015. 31(2): p. 1219-1221.
15. McMurdie, H.F., et al., Standard X-ray diffraction powder patterns from the JCPDS research associateship. Powder Diffraction, 1986. 1(2): p. 64-77.
16. Geetha, M., H. Nagabhushana, and H. Shivananjaiah, Green mediated synthesis and characterization of ZnO nanoparticles using Euphorbia Jatropa latex as reducing agent. Journal of Science: Advanced Materials and Devices, 2016. 1(3): p. 301-310.

17. Gosens, I., et al., Impact of agglomeration state of nano-and submicron sized gold particles on pulmonary inflammation. Particle and fibre toxicology, 2010. 7(1): p. 1-11.
18. Donga, S. and S. Chanda, Caesalpinia crista seeds mediated green synthesis of zinc oxide nanoparticles for antibacterial, antioxidant, and anticancer activities. BioNanoScience, 2022. 12(2): p. 451-462.
19. Sampath, S., et al., Facile green synthesis of zinc oxide nanoparticles using Artocarpus hirsutus seed extract: spectral characterization and in vitro evaluation of their potential antibacterial-anticancer activity. Biomass Conversion and Biorefinery, 2023: p. 1-15.
20. Anthony, E.T., N.A.J.E.S. Oladoja, and P. Research, Process enhancing strategies for the reduction of Cr (VI) to Cr (III) via photocatalytic pathway. 2022. 29(6): p. 8026-8053.
21. Shao, D., et al., Photocatalytic reduction of Cr (VI) to Cr (III) in solution containing ZnO or ZSM-5 zeolite using oxalate as model organic compound in environment. 2009. 117(1-2): p. 243-248.
22. Liu, W., J. Ni, and X.J.W.r. Yin, Synergy of photocatalysis and adsorption for simultaneous removal of Cr (VI) and Cr (III) with TiO2 and titanate nanotubes. 2014. 53: p. 12-25.
23. Sibhatu, A.K., et al., Photocatalytic activity of CuO nanoparticles for organic and inorganic pollutants removal in wastewater remediation. 2022: p. 134623.